

Measurement of J/ψ , Υ and b hadron production in proton-proton collisions at $\sqrt{s} = 7$ TeV with CMS

Nuno Leonardo*

on behalf of the CMS Collaboration

Purdue University

E-mail: Nuno.Leonardo@cern.ch

The CMS experiment is collecting data from LHC proton-proton collisions, with high performance. In the first months of LHC operation, CMS has placed considerable emphasis on heavy flavor and quarkonium physics, exploring in particular low-threshold muon triggers with affordable event rates. The first 300 nb^{-1} of data accumulated by the experiment have been thoroughly explored to establish the overall good performance of the detector, and extract initial physics results. The first measurements of the J/ψ , Υ and b hadron production cross sections in proton-proton collisions at 7 TeV are presented in this paper. Comparisons with model predictions are also shown.

*35th International Conference of High Energy Physics - ICHEP2010,
July 22-28, 2010
Paris France*

*Speaker.

1. Introduction

The dataset collected by the CMS experiment in the initial months of LHC operation is used to extract the first heavy flavor measurements in proton-proton collisions at $\sqrt{s} = 7$ TeV. These measurements serve in addition to establish the good performance of the detector.

2. Di-muon resonances

A description of the CMS detector is provided elsewhere [1]. Muons are identified as tracks that are reconstructed in the inner silicon tracker which are associated to compatible signals in the outer muon spectrometer [2]. A relative momentum resolution better than $\mathcal{O}(2\%)$ is achieved for transverse momenta p_T smaller than 100 GeV/c [3]. The identified dimuon resonances in the full mass spectrum are shown in Fig. 1 (where the variable bin size is $\text{mass} \times 1\%$).

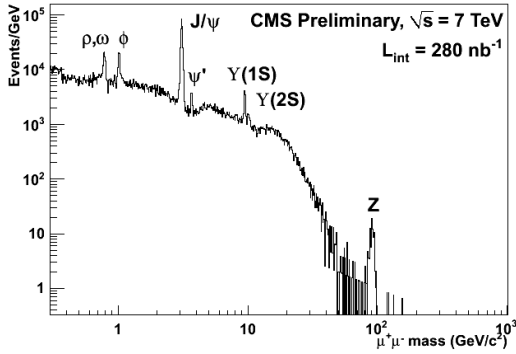


Figure 1: Di-muon mass spectrum.

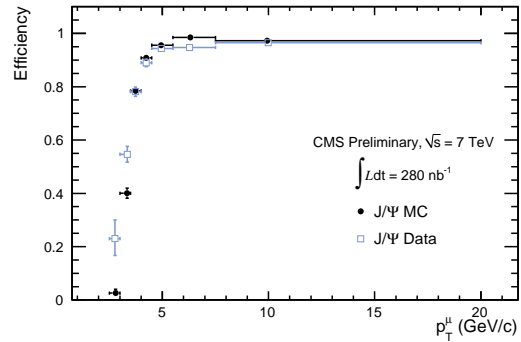


Figure 2: Muon trigger efficiency ($|\eta^\mu| < 1.2$).

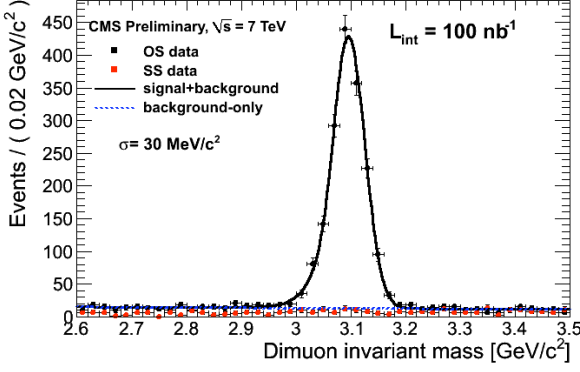
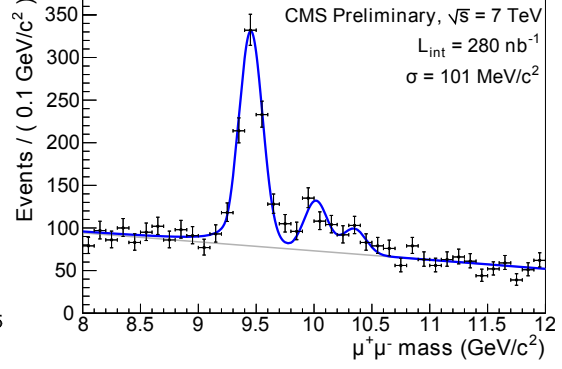
The triggers employed for online selection contain paths with relatively loose requirements, allowing to collect events down to very low momenta. These include single-muon paths with thresholds as low as 3 GeV/c, and double-muon paths with no explicit p_T thresholds, which are employed in the measurements here described.

Muon reconstruction and trigger efficiencies (ϵ) are determined directly from the data sample, using a tag-and-probe procedure applied to the more abundant J/ψ resonance. The efficiency of the referred double-muon trigger is shown in Fig. 2 for a single-leg (probe) muon.

3. Quarkonia

Selection of charmonium and bottomium states is based on opposite-sign dimuon events, where the branching fractions $\mathcal{B}(\mu^+\mu^-)$ are about 6% (J/ψ) and 2% (Υ). Loose quality criteria are imposed on number of hits in the tracker systems, muon track fit quality, and vertex probability. Pseudorapidity-dependent muon p_T thresholds are further applied to ensure the dimuon state is reconstructed well within the detector geometric and kinematic acceptance \mathcal{A} .

About 12 000 (1 000) J/ψ (Υ) signal candidates are reconstructed in a 100nb^{-1} (280nb^{-1}) dataset. The invariant mass distributions for candidates reconstructed in the central detector region are shown in Figs. 3 and 4.

Figure 3: Mass distribution of J/ψ candidates.Figure 4: Mass distribution of $\Upsilon(nS)$ candidates.

4. Υ production cross section

The differential cross section in transverse momentum, $\frac{d\sigma}{dp_T}$, is determined as

$$\frac{d\sigma}{dp_T} \times \mathcal{B}(\mu^+\mu^-) = \frac{N_{\text{corr}}(p_T; \mathcal{A}, \varepsilon)}{\mathcal{L} \cdot \Delta p_T}, \quad (4.1)$$

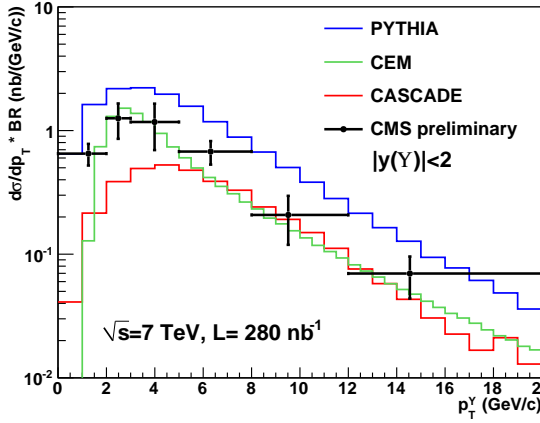
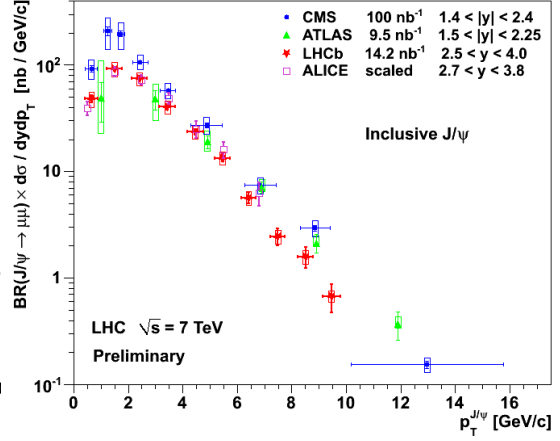
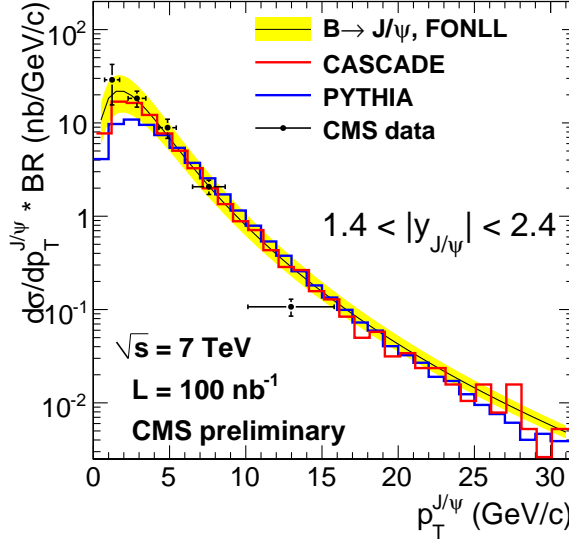
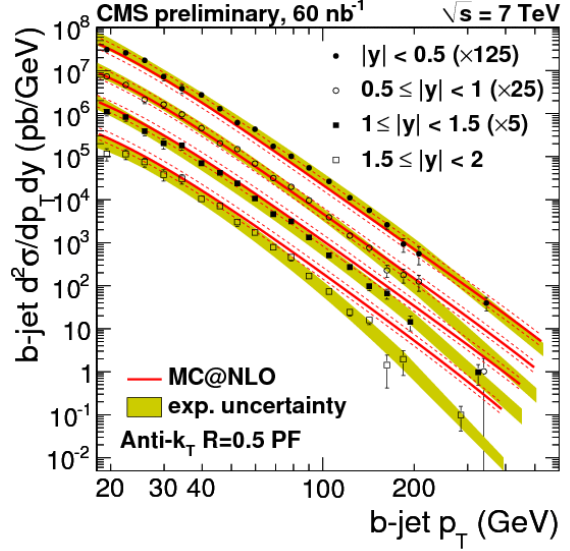
where N_{corr} is the corrected signal yield, obtained from an acceptance \mathcal{A} and efficiency ε weighted fit to the dimuon mass distribution, measured in a p_T interval of width Δp_T . Event weights are given by $(\mathcal{A}\varepsilon)^{-1}$. \mathcal{L} denotes the integrated luminosity of the dataset.

The acceptance \mathcal{A} is strongly affected by the quarkonia polarization. This observable will require an enlarged dataset to be extracted, and has otherwise not been satisfactorily established to date. In the null polarization scenario, the $\Upsilon(1S)$ cross section [4] is measured to be $\sigma \cdot \mathcal{B} = (8.3 \pm (0.5)_{\text{stat.}} \pm (0.9)_{\text{lumi.}} \pm (1.0)_{\text{syst.}})$ nb, in the rapidity interval $|y| < 2$. The differential cross section is displayed and compared to theory predictions in Fig. 5. The dominant systematic uncertainty arises from the muon efficiency measurements. Extreme polarization assumptions induce $\sim 20\%$ -level variations. The cross section ratio $(\Upsilon(2S) + \Upsilon(3S))/\Upsilon(1S)$ is measured to be $0.44 \pm (0.06)_{\text{stat.}} \pm (0.07)_{\text{syst.}}$.

5. J/ψ production cross section

The J/ψ differential cross section is measured similarly as in Eq. 4.1. In the null polarization scenario, the total inclusive J/ψ cross section [5], measured in the range $|y| < 2.4$, is $\sigma \cdot \mathcal{B} = (289.1 \pm (16.7)_{\text{stat.}} \pm (60.1)_{\text{syst.} \oplus \text{lumi.}})$ nb. As in Sec. 4, the dominant systematics contribution arises from the tag-and-probe efficiency determination, and polarization effects can induce up to 20% variations. The p_T differential results are displayed in Fig. 6. A comparison to preliminary results shown by other LHC experiments [6] in this conference is also displayed.

The fraction of J/ψ from b -hadron decays is extracted from a two-dimensional fit to the dimuon mass and pseudo-proper decay time, $t = L_{xy} \cdot m_{J/\psi} / p_T$, where L_{xy} is the transverse displacement between the dimuon and the primary interaction vertices. The differential cross section of non-prompt J/ψ production is shown in Fig. 7. The total cross section result yields $\sigma \cdot \mathcal{B} = (56.1 \pm (5.5)_{\text{stat.}} \pm (7.2)_{\text{syst.} \oplus \text{lumi.}})$ nb.


 Figure 5: $\Upsilon(1S)$ p_T differential cross section.

 Figure 6: Inclusive J/ψ differential cross section.

 Figure 7: Non-prompt J/ψ differential cross section ($1.4 < |y(J/\psi)| < 2.4$).

 Figure 8: b -jets double differential cross section.

6. Inclusive b production cross section

Two additional, complementary methods have been employed for investigating the inclusive b production cross section. One approach exploits the decay $b \rightarrow \mu + X$, and the muon transverse momentum component p_T^{rel} relative to the the b flight direction, as the b discriminating observable [7]. The p_T^{rel} distribution is fit to two templates: one for b and c quarks, extracted from simulation, and another for light quarks and gluons ($udsg$), obtained from an inclusive jets data sample. Using 8.1 nb^{-1} of data, the measured total inclusive b -hadron cross section, for $p_T^\mu > 6 \text{ GeV}/c$ and $|\eta^\mu| < 2.1$ is $(1.48 \pm (0.04)_{\text{stat.}} \pm (0.22)_{\text{syst.}} \pm (0.16)_{\text{lumi.}}) \mu\text{b}$. The systematic uncertainty is dominated by the description of the background.

Another approach, covering a higher momentum range, exploits a b tagging technique based on secondary vertex identification [8]. The estimated b tagging efficiency varies from 10%, for $p_T \sim 20$ GeV/c, to 60%, for $p_T \sim 100$ GeV/c, while the contamination from c and $udsg$ jets results in a mistag rate of $\sim 10\%$. The differential cross section in rapidity and transverse momentum is shown in Fig. 8. The leading systematic uncertainty arises from data-based constraints on the b tagging efficiency (20%).

7. Conclusions

The inclusive b , J/ψ and Υ production cross sections at $\sqrt{s} = 7$ TeV have been measured for the first time. The results demonstrate an excellent performance of the CMS detector.

References

- [1] CMS Coll., JINST 0803:S08004 (2008)
- [2] CMS Coll., CMS PAS MUO-10-002
- [3] CMS Coll., CMS PAS TRK-10-004
- [4] CMS Coll., CMS PAS BPH-10-003
- [5] CMS Coll., CMS PAS BPH-10-002
- [6] ALICE, ATLAS, and LHCb Collaborations, preliminary results presented at this conference
- [7] CMS Coll., CMS PAS BPH-10-007
- [8] CMS Coll., CMS PAS BPH-10-009